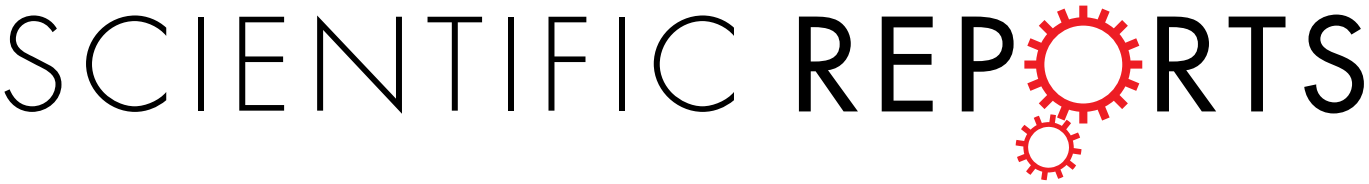

OPEN

Neuronal entry and high neurotoxicity of botulinum neurotoxin A require its N-terminal binding sub-domain

Received: 23 June 2016
Accepted: 09 February 2017
Published: 15 March 2017

Jiafu Wang*, Jianghui Meng*, Marc Nugent, Minhong Tang & J. Oliver Dolly

Botulinum neurotoxins (BoNTs) are the most toxic proteins known, due to inhibiting the neuronal release of acetylcholine and causing flaccid paralysis. Most BoNT serotypes target neurons by binding to synaptic vesicle proteins and gangliosides via a C-terminal binding sub-domain (H_{CC}). However, the role of their conserved N-terminal sub-domain (H_{CN}) has not been established. Herein, we created a mutant form of recombinant BoNT/A lacking H_{CN} ($rA\Delta H_{CN}$) and showed that the lethality of this mutant is reduced 3.3×10^4-fold compared to wild-type BoNT/A. Accordingly, low concentrations of $rA\Delta H_{CN}$ failed to bind either synaptic vesicle protein 2C or neurons, unlike the high-affinity neuronal binding obtained with ^{125}I-BoNT/A ($K_d = 0.46$ nM). At a higher concentration, $rA\Delta H_{CN}$ did bind to cultured sensory neurons and cluster on the surface, even after 24 h exposure. In contrast, BoNT/A became internalised and its light chain appeared associated with the plasmalemma, and partially co-localised with vesicle-associated membrane protein 2 in some vesicular compartments. We further found that a point mutation (W985L) within H_{CN} reduced the toxicity over 10-fold, while this mutant maintained the same level of binding to neurons as wild type BoNT/A, suggesting that H_{CN} makes additional contributions to productive internalization/translocation steps beyond binding to neurons.

Botulinum neurotoxins (BoNTs) are life-threatening proteins that potently and specifically bind to certain peripheral nerve endings and block the exocytotic release of transmitters. Exploiting their high specificity for cholinergic nerves, the large complex of BoNT/A containing haemagglutinin and other non-toxic proteins isolated from *Clostridium botulinum*, and to a lesser extent the type B counterpart, has proved successful in treating hyper-excitability disorders of muscles and secretory glands[1]. Also, the /A complex has been used for aesthetic/facial applications[2,3]. Furthermore, it benefits patients who suffer from certain types of migraine/headache[4] due, at least in part, to blockade by BoNT/A or its complex of the exocytosis of substance P and calcitonin gene-related peptide from sensory fibres[5–7]. Recently, BoNT/A was reported to block tumour necrosis factor alpha (TNF-α) induced surface trafficking in sensory neurons of transient receptor potential (TRP) A1 and V1 channels; accordingly, enhancement by TNF-α of Ca^{2+} influx through these upregulated surface channels is abolished[8].

All 7 serotypes of BoNTs (/A–/G) are mainly produced by the different types of *Clostridium botulinum* as single polypeptide chains (SC) (Mr ~ 150 k). Each is activated by *Clostridial* or host cell proteases to the highly-potent dichain (DC) form; this consists of an N-terminal ~50 k Zn^{2+}-metalloprotease light chain (LC) linked to a 100 k heavy chain (HC) via a disulphide and non-covalent bonds. The crystal structures of BoNT/A, /B and /E have a tri-modular architecture[9–11], with each serving a 'chaperone-like' role for the other domains. BoNT/A and /B are known to undergo acceptor-mediated endocytosis[12], following binding to polysialo-gangliosides and synaptic vesicle proteins via the C-terminal half of HC (H_C)[13,14]. Uptake of BoNT/A and /B into resting neurons[15] requires lipid rafts, binding to their respective acceptors, synaptic vesicle protein 2 (SV2) and synaptotagamin, and passage through acidic compartments[16]. K^+-depolarisation of cultured neurons recruits several endocytosis-promoting proteins (e.g. dynamin, clathrin, adaptor protein complex-2 and amphiphysin), thereby, enhancing toxin internalisation[16]. An acidic environment inside the vesicles induces the N-terminal half of HC (H_N) to form a channel which allows the LC of each to unfold and cross the limiting membrane. In the cytosol,

International Centre for Neurotherapeutics, Dublin City University, Glasnevin, Dublin 9, Ireland. *These authors contributed equally to this work. Correspondence and requests for materials should be addressed to J.W. (email: jiafu.wang@dcu.ie)

they regain enzymically-active structures and separate from their HC after reduction of the inter-chain disulphide[17]. Inhibition of thioredoxin reductase located on the synaptic vesicles prevents the paralysis induced by BoNTs[18]. The LCs cleave soluble N-ethylmaleimide-sensitive factor attachment protein receptors (SNAREs) [reviewed by refs 1 and 17]. The presence of a di-leucine motif in the LC of BoNT/A is responsible for it displaying the long-lasting duration of action in motor nerves[19], due to persistently truncating synaptosomal-associated protein of 25 k (SNAP-25). This substrate is also susceptible to BoNT/E and /C1; the latter additionally truncates syntaxin, whereas BoNT/B, /D, /F and /G cleave vesicle-associated membrane proteins (VAMPs) at distinct bonds [reviewed in ref. 1]. Truncations of these SNARE proteins block fusion of synaptic vesicles and, hence, neurotransmitter release.

Significant advances have been made in identifying acceptors that bind to the C-terminal sub-domain of H_C (H_{CC}) of BoNTs, and deciphering molecular details of their interactions. In addition to gangliosides, SV2 was discovered as an acceptor for /A, /D, /E and /F whereas synaptotagmin I and II serve this role for /B and /G [reviewed in refs 1 and 17]. Fibroblast growth factor receptor 3 (FGFR3) has also been reported to bind BoNT/A[20]. A high-resolution crystal structure of full-length BoNT/B complexed with the recognition domain of its acceptor revealed that the helix of synaptotagmin II binds to a saddle-shaped crevice at the C-terminal end of the H_{CC}; this locus is adjacent to the non-overlapping ganglioside-binding site of BoNT/B[13,14]. Binding to the ganglioside GT1b also enables BoNT/B to sense low pH for directing formation of a translocation channel[21]; binding of both synaptotagmin II and gangliosides underlies its high selectivity and affinity. Recently, the crystal structures of H_C from BoNT/A bound to glycosylated and non-glycosylated SV2C-L4 were solved[22,23]. In addition to residues in H_{CC}, several amino acids in H_{CN} were also reported to interact with N559 glycan in SV2C and contribute to binding to neurons[23]. It is noted that BoNT/D uses SV2s as receptors and enters neurons independently of the status of glycosylation of SV2[23]. This raises the possibility that H_{CN} may serve additional roles e.g. binding to unknown receptors, aiding internalisation and facilitating the channel formation for translocation of protease. H_{CN} is known to adopt a β-sheet jelly roll fold[24], bind to micro-domains of the plasma membrane and interact with phosphatidylinositol phosphates[25]. The crystal structure has been reported of a BoNT mosaic serotype C/D with tetraethylene glycol (PG4)[26], a moiety thought to mimic the hydrophobic fatty acid tails of phospholipids. Therefore, it was hypothesised that H_{CN} might be involved in interacting with phospholipid on the neuronal membrane[26]. Nevertheless, the functional role of H_{CN} in the multi-phasic action of BoNTs remains to be established.

Herein, the H_{CN} of BoNT/A is demonstrated to make an essential contribution to its extremely high lethality; the latter is dramatically decreased upon deleting this sub-domain. Recombinant BoNT/A devoid of the H_{CN} ($rA\Delta H_{CN}$) virtually fails to truncate intra-neuronal SNAP-25. This is due to a lack of high-affinity ($K_D = 0.46$ nM) binding to neurons seen with ^{125}I-radiolabelled BoNT/A. Although a higher concentration of $rA\Delta H_{CN}$ did interact with neurons, the majority failed to get internalised as revealed using novel engineered tagged-derivatives. Furthermore, full-length BoNT/A containing a mutated H_{CN} residue (Trp 985) retains high-affinity neuronal binding but exhibits significantly reduced ability to cleave intra-neuronal target. Therefore, we have deduced that H_{CN} is involved in binding to neurons and entry of BoNT/A leading to proteolytic inactivation of SNAP-25.

Results

Recombinantly-produced BoNT/A (rA) with its H_{CN} sub-domain deleted exhibits unaltered protease activity. To investigate the role of H_{CN}, nucleotides encoding residues (I874-Q1091) were first deleted (Fig. 1a) from a pET29a-BoNT/A gene construct, previously described[19]. The resultant construct was transformed into *E. coli* for expression, by auto-induction. The deleted variant protein ($rA\Delta H_{CN}$) was fully purified as a SC protein using immobilised metal affinity chromatography (IMAC), followed by anion-exchange chromatography as for rA (Fig. S1). Note there was no significant difference in terms of yield (~5 mg/L culture) and purity between $rA\Delta H_{CN}$ and rA. After incubation with thrombin, the $rA\Delta H_{CN}$ SC was converted to a DC form with an expected Mr (~125 k); its constituent LC (~50 k) and H_N-H_{CC} (~75 k) were separated by SDS-PAGE only in the presence of reducing agent, confirming that the inter-chain disulphide had been formed in the expressed protein (Fig. 1b). Retention by $rA\Delta H_{CN}$ of proteolytic activity was confirmed towards a recombinant model substrate (GFP-SNAP-25C_{73}-His_6)[27,28] showing a similar EC_{50} value to rA (Fig. 1c). Therefore, it is clear that deleting H_{CN} from BoNT/A does not affect the enzyme activity of its integral LC.

Deletion of H_{CN} from BoNT/A significantly decreases its intra-neuronal cleavage of SNAP-25 and lethality. The combined functional properties of $rA\Delta H_{CN}$ were examined following exposure to rat cultured cerebellar granule neurons (CGNs), with subsequent monitoring of SNAP-25 truncation. This reflects the extent of internalisation and translocation of LC into cytosol where it acts on its target. Overnight incubation of 1 nM $rA\Delta H_{CN}$ with the cultured neurons resulted in only a small fraction of SNAP-25 being cleaved, which equates to the amount produced by as little as 0.1 pM of wild-type (WT) rA (Fig. 2a). Extrapolation of this data revealed that deleting H_{CN} caused ~10^4-fold drop in SNAP-25 cleavage (Fig. 2b). Similar results were obtained upon comparing SNAP-25 cleavage by rA and $rA\Delta H_{CN}$ after overnight exposure to rat cultured trigeminal ganglion neurons (TGNs); again, deletion of H_{CN} resulted in ~10^4-fold decrease in the degree of SNAP-25 cleavage (Fig. 2c and d). As $rA\Delta H_{CN}$ and rA displayed similar protease activity *in vitro* towards a recombinant substrate (cf. Fig. 1c), it is reasonable to suspect that this dramatic decrease in SNAP-25 cleavage arose from defective internalisation and/or translocation of LC to the cytosol. The *in vitro* data concur with the results observed *in vivo*; intra-peritoneal injection of as much as 167 ng of $rA\Delta H_{CN}$ was needed to kill 50% of the mice, corresponding to a toxicity of 6×10^3 lethal doses (LD_{50})/mg. This is ~3.3×10^4-fold lower than that for its WT (Fig. 2e). Thus, it was necessary to inject a ~33,400-fold larger quantity of $rA\Delta H_{CN}$ than rA to induce muscle weakening to a similar extent (Fig. 2f); administering 10 or 1 ng of $rA\Delta H_{CN}$ failed (data not shown) to induce a measurable digit

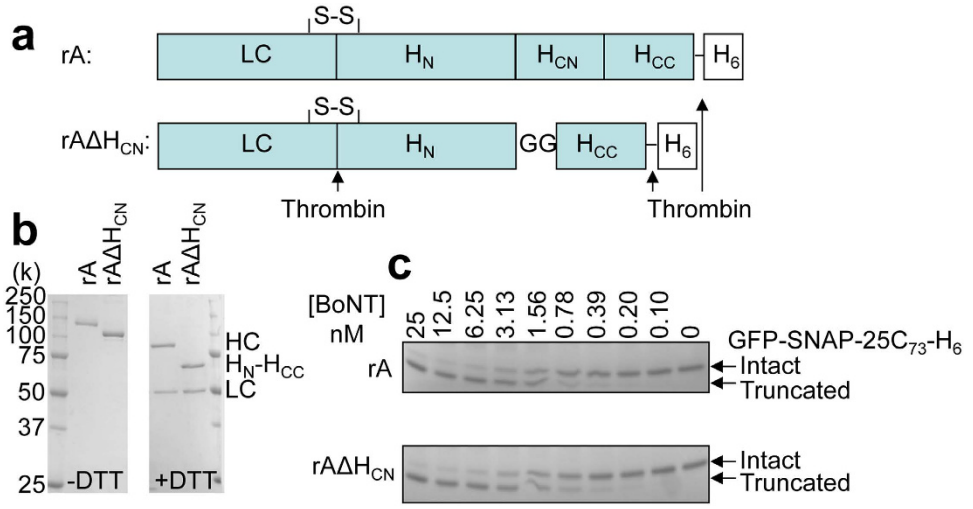

Figure 1. Expressed, purified $rA\Delta H_{CN}$ and rA showed similar proteolytic activity. (**a**) Schematic of rA and $rA\Delta H_{CN}$. Nucleotides encoding I_{874}-Q_{1091}were deleted and replaced with 6 nucleotides GGCGGT to generate $rA\Delta H_{CN}$. S-S denotes inter-chain disulphide, GG between H_N and H_{CC} in $rA\Delta H_{CN}$ represent glygly residues. H_6 indicates 6xHis and (↑) represent consensus site for thrombin. (**b**) $rA\Delta H_{CN}$ and rA expressed in *E. coli*, purified and nicked before being subjected to SDS-PAGE in the presence or absence of DTT, followed by Coomassie staining. Note that HC and H_N-H_{CC} were separated from LCs only under reducing conditions. (**c**) $rA\Delta H_{CN}$ and rA exhibited similar protease activity towards a model GFP-SNAP-25C_{73}-His_6 substrate.

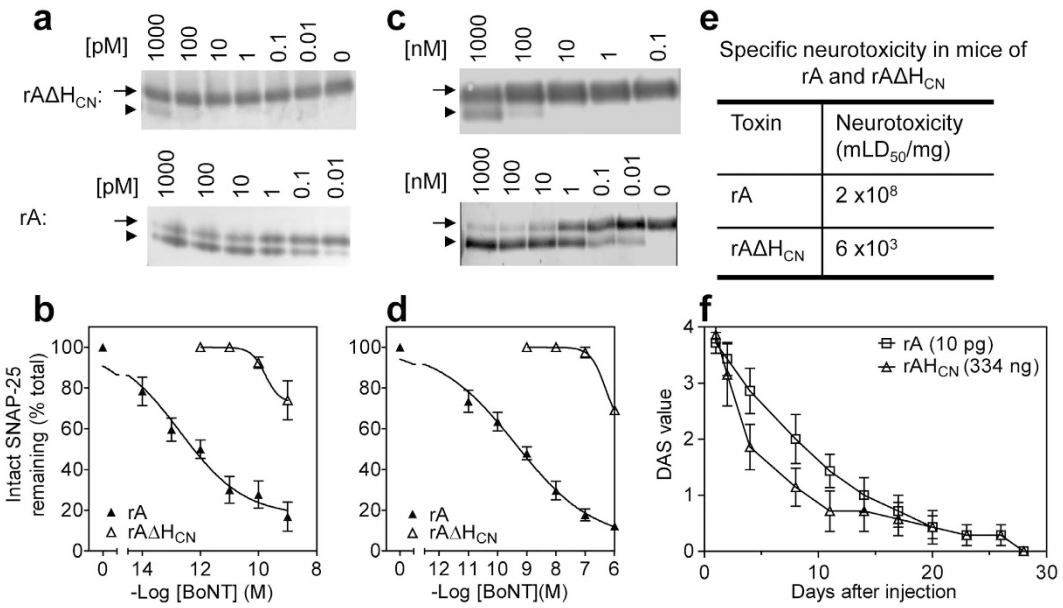

Figure 2. $rA\Delta H_{CN}$ caused minimal cleavage of neuronal SNAP-25 and displayed greatly reduced lethality. Rat cultured CGNs (**a**,**b**) or TGNs (**c**,**d**) were incubated with various concentrations of rA or $rA\Delta H_{CN}$ in medium for 24 h before harvesting in LDS sample buffer. Samples were separated by SDS-PAGE followed by Western blotting with an antibody recognising both intact and cleaved SNAP-25. The arrow and arrowhead in panel a and c indicate intact and cleaved SNAP-25, respectively. Data are mean ± S.E.M, n = 3. (**e**) Removal of the H_{CN} sub-domain from rA dramatically reduced its lethality in mice. (**f**) DAS values were recorded over 28 days after injecting rA or $rA\Delta H_{CN}$ into the right gastrocnemius muscle of mice; SEM values are shown from 7 mice for each toxin. Two-way ANOVA with Bonferroni post hoc test analysis highlights that there is no significant difference ($p > 0.05$ at all time points) between the curves for rA and a 33,400-fold higher quantity of $rA\Delta H_{CN}$.

abduction score (DAS)[29]. Our collective findings highlight the dramatic loss in the overall biological activity upon deleting the H_{CN} from rA.

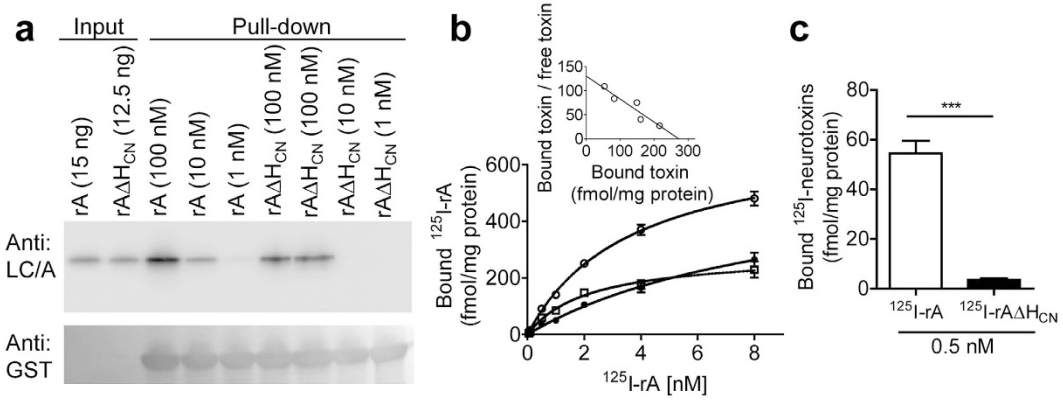

Figure 3. Deletion of H_{CN} from rA diminished its binding to SV2C-L4 and intact neurons. (**a**) Western blot from the *in vitro* pull-down assay (see Materials and Methods) shows that rAΔH_{CN} at 10 and 1 nM concentrations failed to bind non-glycosylated GST-SV2C-L4, in contrast to rA. At 100 nM, a lower amount of rAΔH_{CN} than rA was retained by immobilised SV2C-L4. Note that samples were reduced by DTT before SDS-PAGE. (**b**) CGNs were incubated with increasing concentrations of ^{125}I-rA alone (○) or with 1 μM BoTIM/A (●) for 1 h at 4 °C followed by three washes before γ counting of the pellets. Subtracting non-saturable binding (●) from the total binding (○) yielded the saturable component (□). Inset: Scatchard plot of the saturable binding of ^{125}I-BoNT/A to CGNs. (**c**) Binding of ^{125}I-labelled rAΔH_{CN} to CGNs, measured as in (**b**) was non-significant. Data are mean ± S.E.M from two independent experiments performed in duplicates.

Low concentrations of rAΔH_{CN} fail to bind SV2C and intact neurons. To decipher the detrimental effects of deleting H_{CN}, the first step of the intoxication process was examined. For assessing whether deletion of H_{CN} from rA alters its binding to the known protein acceptor, a well-established albeit qualitative pull-down assay was performed, using immobilised the bacterially-expressed fourth loop (L4) of SV2C (residues 454–580) fused to glutathione S-transferase (GST)[30–32]. rAΔH_{CN} gave undetectable binding to this non-glycosylated SV2C at 1 or 10 nM, unlike rA (Fig. 3a). In contrast, binding of a high concentration of rAΔH_{CN} (100 nM) was observed, but at reduced levels compared to rA (Fig. 3a). For more in-depth analysis of the binding of rA and rAΔH_{CN} to CGNs, a sensitive and quantitative isotope assay was employed. rA and rAΔH_{CN} were labelled with [^{125}I]iodine to high specific activities (920 and 840 Ci/mmol, respectively), using an established chloramine-T method[33]. Incubation of increasing concentrations of ^{125}I-rA with CGNs revealed that the level of saturable binding reached a plateau at 8 nM, which was calculated by subtracting non-saturable binding in the presence of 1 μM unlabelled protease-inactive form of BoNT/A (BoTIMA)[19] from the total binding (Fig. 3b). Scatchard analysis (Fig. 3b inset) revealed high-affinity binding of ^{125}I-rA to CGNs ($K_d = 0.46 \pm 0.03$ nM from two independent experiments), which is similar to the value of ^{125}I-labelled native BoNT/A binding to rat brain synaptosomal membranes[33]. Notably, deletion of H_{CN} from ^{125}I-rA drastically reduced its ability to bind to CGNs (Fig. 3c).

A high concentration of rAΔH_{CN} binds but fails to enter into neurons. In addition to the above-noted absence of high-affinity binding upon deleting rAΔH_{CN}, it was pertinent to establish whether this deletion inhibited internalisation of toxin bound at a higher concentration. To permit monitoring of the trafficking, tagged variants were engineered by incorporating a haemagglutinin (HA) epitope before the thrombin recognition sequence in the loop region of rA and rAΔH_{CN} (Fig. 4a). This allowed their respective locations to be visualised by means of a commercially-available antibody for recognising HA. Incorporation of HA did not affect the expression pattern, purity (Fig. 4b), yield or protease activity of either rA or rAΔH_{CN} (data not shown). As expected, anti-HA antibody only recognised the LCs with HA tag in rA-HA and rAΔH_{CN}-HA but not the wild-type (WT) LC in rA (Fig. 4c). The larger size of TGNs (soma diameter ~25 μm) compared to that of CGNs (~6 μm) facilitated more clear-cut cellular localization of the tagged toxins. Immuno-cytochemistry and confocal microscopy of cultured TGNs, incubated for 24 h with 100 nM rA-HA followed by fixation and permeabilisation, revealed labelling associated with the plasma membrane (possibly the inner side) and some vesicular regions in the cell body (Fig. 5a). Punctate staining was also observed along the neurites, to some extents co-localised with VAMP2 (Fig. 5a), a vesicle marker. Again, this HA antibody could not visualise WT BoNT/A devoid of the tag (Fig. 5b), confirming its specificity. A majority of rAΔH_{CN} appeared clustered at the plasma membrane, and on neurites, even after 24 h incubation (Fig. 5c and Fig. S2). Similar experiments repeated except omitting permeabilisation indicated punctate labelling with rAΔH_{CN}-HA on the outer surface of cell body and neurites, revealed using anti-HA antibody (Fig. S2). Moreover, TGNs incubated with 100 nM rAΔH_{CN}-HA and an excess (1 μM) of non-tagged rAΔH_{CN} in high (60 mM) K^+ (HK) buffer[16] for 10 min exhibited reduced labelling of neurites compared to that treated with tagged toxin only (Fig. S3). Thus, rAΔH_{CN} seems unable to enter neurons even when a high concentration had to be employed to achieve binding.

Tryptophan 985 in the H_{CN} of BoNT/A contributes to its neuronal internalisation/protease translocation steps. In search of key residues in H_{CN} of full-length BoNT/A which might contribute to entry resulting from its binding to acceptor, residues thought pertinent to PG4 interaction (see Introduction) were mutated. A series of 8 constructs were made containing 1 or 2 mutations such as $F_{941}A$, $W_{974}L$, $W_{985}L$,

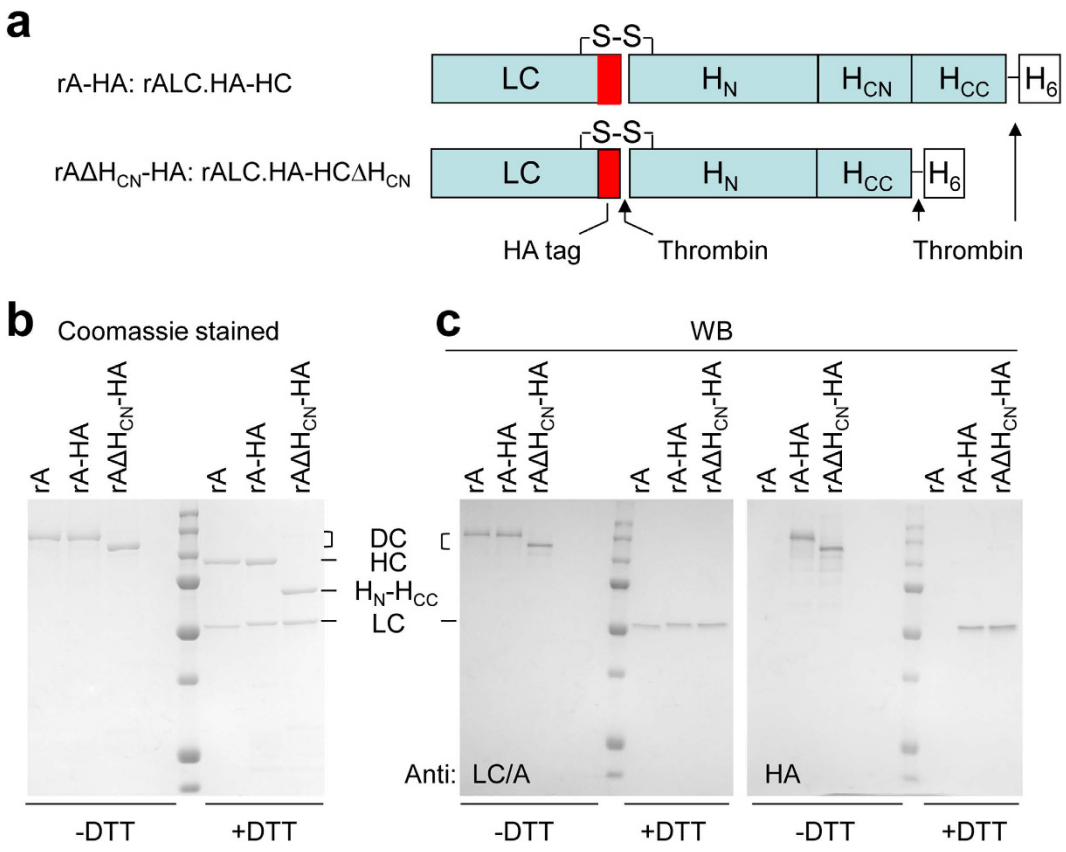

Figure 4. Generation of probes for visualising the cellular location of rAΔH$_{CN}$ and rA. (**a**) Schematic of the BoNT/A probes generated. A short length of nucleotides encoding the HA tag was inserted before the thrombin cleavage site in the loop region of rA and rAΔH$_{CN}$ to yield constructs encoding rA LC.HA-HC and rA LC.HA-H$_N$H$_{CC}$. For simplicity, the latter two were termed rA-HA and rAΔH$_{CN}$-HA, respectively. After purification, nicked rA-HA and rAΔH$_{CN}$-HA were subjected to SDS-PAGE in the presence or absence of DTT, followed by Coomassie staining (**b**) and Western blotting, using the indicated antibodies (**c**). rA was loaded for comparison. HA antibody only recognised LCs containing the HA tag. Note that due to the insertion of HA tag, LC-HA migrated slightly slower than WT LC.

W985F, L$_{987}$A, W$_{985}$L/L$_{987}$A, N$_{1021}$A or L$_{1074}$A. The resultant constructs were transformed into *E. coli* for expression; IMAC was used to purify the recombinant mutated and WT proteins. Curiously, no intact protein was obtained for the W985F mutant. Incubation of other mutants or WT with thrombin converted a majority of the SC to the DC form (Fig. 6a). The final yield of single (W$_{974}$L) or double (W$_{985}$L/L$_{987}$A) mutants was decreased by ~10- and 5-fold compared to WT, respectively, whereas the others expressed to levels similar to that of the WT. For standardised measurement of the functionality of each partially purified mutant, their concentrations were adjusted according to that of intact DC rather than total concentration, using WT DC as reference. Initial attempts made to assess if PG4 binds rA proved negative, using a dot blot assay (Fig. S4). Likewise, pre-incubation of 100 pM rA with 1 μM PG4 did not affect subsequent cleavage of intra-neuronal SNAP-25 (Fig. S4).

To evaluate the multiple activities (e.g. acceptor binding/internalisation/cytosolic translocation i.e SNAP-25 cleavage) of the mutants, CGNs were cultured and incubated with WT or each variant at various doses in culture medium for 24 h at 37 °C. This revealed a mild drop in activity of mutant L$_{987}$A (Fig. 6b,c). Changing W$_{974}$ to L did not seem to affect the overall functioning of BoNT/A (dose response curve is near identical to WT: Fig. 6c). Similarly, mutating N$_{1021}$ to A failed to alter SNAP-25 cleavage whereas mutant F$_{941}$A and L$_{1074}$A exhibited minimal decreases in their activities (Fig. S5). The cleavage of SNAP-25 in CGNs dropped over 10-fold after a single (W$_{985}$ to L) or double mutation (W$_{985}$ to L and L$_{987}$ to A) (Fig. 6b,c). The importance of W$_{985}$ for the action of BoNT/A was further investigated by incubating rCGNs with W$_{985}$L mutant or WT for 8 min in low (5 mM) K$^+$ buffer[16]; then, the cells were washed three times to remove unbound toxin and further cultured for 5 h. This mutant gave significant decrease in cleavage of SNAP-25 compared to WT (Fig. 6d,e), but the mutation did not affect its *in vitro* protease activity (Fig. 6f) or binding to non-glycosylated SV2C (Fig. 6g). To investigate whether mutating W985 affects its binding to acceptors on CGNs, this mutant was labelled with ^{125}I to specific activity ~740 Ci/mmol. Notably, ^{125}I-rA(W$_{985}$L) showed near identical binding affinity ($K_d = 0.47 \pm 0.01$ nM from two experiments) (Fig. 6h and inset) as ^{125}I-labelled rA (cf. Fig. 3b). Hence, it is reasonable to deduce that W985 in BoNT/A plays some part in its neuronal internalisation and/or protease translocation after initial binding.

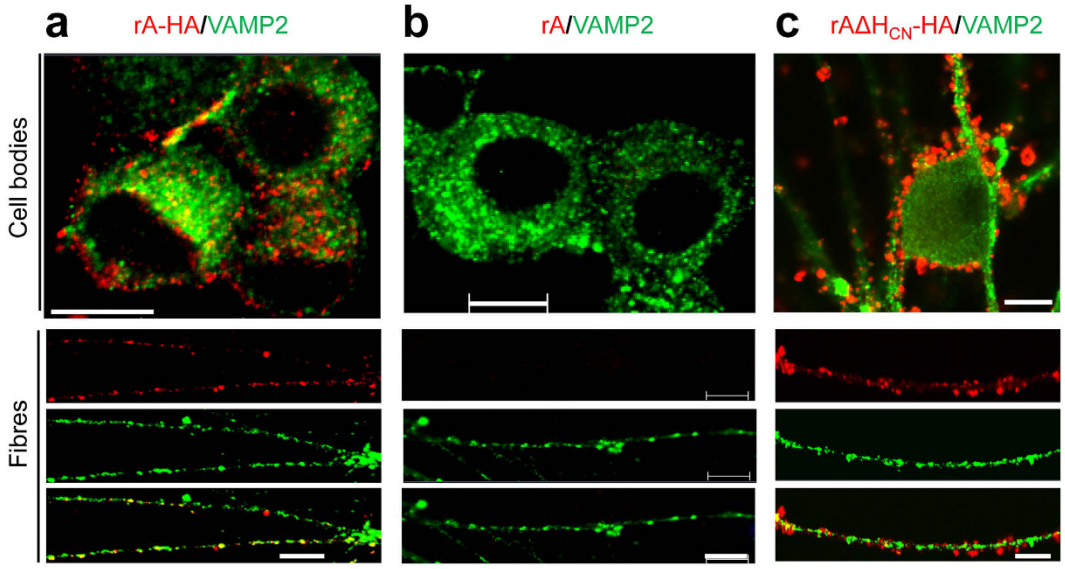

Figure 5. A majority of rAΔH$_{CN}$-HA failed to enter cultured TGNs unlike rA-HA. Rat TGNs on coverslips were incubated with 100 nM of rA-HA (**a**), rA (**b**), or rAΔH$_{CN}$-HA (**c**) for 24 h at 37 °C in culture medium. Washed cells were fixed with paraformaldehyde, permeabilised and blocked with BSA. Paired primary antibodies [rabbit monoclonal anti-HA and mouse monoclonal anti-VAMP2] were added for 1 h. Washed samples were incubated with Alexa Fluor 488 goat anti mouse IgG and Alexa Fluor 568 goat anti-rabbit IgG for 1 h. Images of cell bodies and fibres were captured with a confocal microscope. Representative images from three independent experiments are shown. Bars, 10 μm.

Discussion

It is reported herein that BoNT/A lacking the H$_{CN}$ sub-domain exhibits greatly reduced activity in cleaving intra-neuronal SNAP-25, and dramatically decreased lethality *in vivo*, due to being unable to bind to neurons with high affinity comparable to BoNT/A. Moreover, mutation of W985 reduced the toxicity of BoNT/A.

Research in the last few decades has greatly advanced understanding of the multi-phasic mechanism of action of BoNTs. This includes binding to SV2 (BoNT/A, /D, /E and /F) or synaptotagmin I/II (BoNT/B and /G) via H$_{CC}$ subdomain, acceptor-mediated endocytosis, translocation by the H$_N$, and cleavage of SNAREs by LC[1]. To determine the functional role of the conserved H$_{CN}$, we first deleted this sub-domain from BoNT/A. Although its protease activity *in vitro* was not affected, rAΔH$_{CN}$ failed to cleave the intra-neuronal substrate. This is due to loss of high-affinity binding to neurons, as quantified using the radio-iodinated toxins. Our results accord with a recent elegant report on the crystal structure of H$_C$/A in complex with glycosylated human SV2C[23]. Several residues in H$_{CN}$/A have been identified as being essential for binding and uptake of BoNT/A into neurons[23]. As expected, the neuronal membrane acceptors gave a higher affinity for ^{125}I-rA than reported for glycosylated SV2C-L4 due to use of the full-length protein and endogenous gangliosides. These *in vitro* findings are reconcilable with the decreased ability of rAΔH$_{CN}$ relative to rA to cause muscle weakening, and lethality in mice. We also show that rAΔH$_{CN}$ at a high concentration can still bind but fails to enter into the cultured sensory neurons, suggesting that H$_{CN}$ might additionally contribute to efficient internalisation. However, this requires further investigation.

An earlier study[25] found that H$_{CN}$ binds to PIPs which might allow the subsequent insertion of H$_N$ into the vesicular membrane. Four positively-charged residues in H$_{CN}$/A: Arg-892, Lys-896, Lys-902, Lys-910 were proposed to interact with PIP. However, mutating Arg892 and Lys896 or Lys902 and 910 to Ala in full-length of BoNT/A did not reduce its cleavage of SNAP-25 in cultured CGNs (Fig. S6). Interaction of H$_{CN}$ in the H$_C$ of BoNT mosaic serotype C/D with PG4 was also revealed by the crystal structure[26], and 6 out of the 9 residues contacting PG4 are highly conserved between BoNT serotypes, A-F. Herein, mutating 5 out of 6 of these conserved residues within H$_{CN}$ of BoNT/A only gave negligible or minor reduction in SNAP-25 cleavage. Similarly, pre-incubation of BoNT/A with an excess PG4 had no effect on its activity. Thus, our data do not seem to support the proposed roles of PIPs and PG4 in multi-phasic action of BoNT/A. Nevertheless, mutating W985 to L in full-length BoNT/A did not alter its binding to neurons, but caused over a 10-fold drop in the cleavage of intra-neuronal SNAP-25. Hence, our findings suggest that this residue, and probably others, may facilitate BoNT/A internalisation and/or translocation of the protease after initial acceptor binding.

To exploit the protease of BoNT/A for extended therapeutic applications, various approaches have involved replacement of the H$_C$ domain of /A with moieties capable of targeting particular cell types in the nervous and endocrine systems to inhibit the release of neurotransmitters, hormones, neuropeptides and others[34–37]. An even more advanced hybrid protein was recombinantly created by inserting a modified growth hormone-releasing hormone (GHRH) domain into the loop region between LC and H$_N$ of BoNT/D lacking the entire H$_C$ domain[38]. Binding of this molecule to GHRH receptors *in vivo* leads to inhibition of growth hormone secretion in juvenile rats, eventually resulting in reduced body size, bone and mass acquisition[38]. However, the requirement of hundreds of micrograms of this recombinant protein per kilogram body weight restricts its clinical potential for

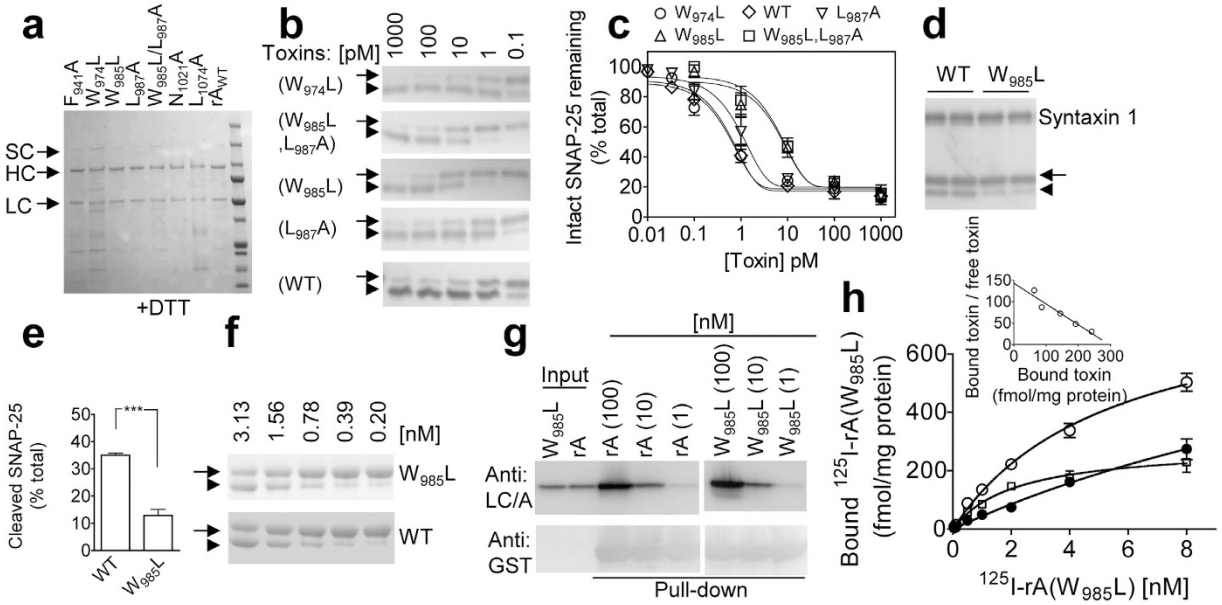

Figure 6. Effects of mutations in the H_{CN} of BoNT/A on its multi-functional activities in rat CGNs as monitored by intracellular cleavage of SNAP-25. (**a**) The expressed and purified mutants were nicked and subjected to SDS-PAGE and Coomassie staining in the presence of DTT; note that thrombin converted the majority of the SC to DC forms. (**b**) After 24 h exposure of CGNs to the different concentrations of the toxin variants in culture medium, the samples were subjected to SDS-PAGE followed by Western blotting. (**c**) Extents of SNAP-25 cleavage in CGNs by $W_{985}L$ and $W_{985}L/L_{987}A$ were decreased > 10-fold compared to that of rA WT. Changing W_{974} to L did not affect the functioning of BoNT/A, whereas mutant $L_{987}A$ exhibited a mild drop in its activity. Note that in some cases error bars are encompassed by symbols. (**d**,**e**) CGNs were treated with 0.5 nM $W_{985}L$ or its WT in 5 mM K^+ (LK) buffer for 8 min at 37 °C. Unbound toxin was removed by three washes before incubation in medium for 5 h to allow internalised toxin to cleave SNAP-25. The arrow and arrowhead in panel b and d indicate intact and cleaved SNAP-25, respectively. Data in panel c and e are mean ± S.E.M, n = 3. ***$P < 0.001$. (**f**) A representative protein stained gel showing BoNT/A WT and $W_{985}L$ mutant have similar protease activities in cleaving GFP-SNAP-$25C_{73}$-His_6 substrate. The arrow and arrowhead indicate intact and cleaved substrate, respectively. (**g**) Non-glycosylated GST-SV2C pulled down BoNT/A WT and $W_{985}L$ variant to similar extents, revealed by Western blotting using antibodies indicated. (**h**) Binding of ^{125}I-rA($W_{985}L$) to CGNs was performed as in Fig. 3b. Subtracting non-saturable binding in the presence of 1 μM unlabelled rA($W_{985}L$) SC (●) from the total (○) yielded the saturable values (□). Inset: Scatchard plot analysis. Data are mean ± S.E.M from two independent experiments performed in duplicates.

treating acromegaly. Improving the potency of the latter and that of the above-mentioned therapeutics is necessary, and would be highly desirable for clinical purposes. Even with very potent BoNT complexes, repeated injections could lead to secondary treatment failure in some patients due to production of neutralizing antibodies[39,40]. To improve the potency of retargeted biotherapeutics, it would be helpful to retain the H_{CN} because, as shown herein, it not only contributes to acceptor binding but also to the internalisation/translocation steps. Of course, whether the targeting moiety and conserved H_{CN} can orchestrate retargeting of the variants into the desired cells await further testing.

Overall, our results reaffirm that each domain of BoNT acts in a 'chaperone-like' fashion for the others. Continued molecular definition of the function of each moiety, and yet to be identified factors, involved in its multi-step intoxication will not only shed insights into pathogenic mechanisms but also help in the design of more effective inhibitors to counteract botulism, as well as in the development of novel therapeutics for other hyper-secretory disorders.

Materials and Methods

Materials. Rabbit monoclonal anti-HA was purchased from Cell Signalling Technology (local distributor, Brennan and Company, Stillorgan, Ireland), and mouse monoclonal anti-VAMP2 from Synaptic System GmbH (Goettingen, Germany). Alexa Fluor 488 goat anti-mouse IgG, Alexa Fluor 488 and 568 goat anti-rabbit IgGs were obtained from Jackson ImmunoResearch (Hamburg, Germany) and Bio-Science (Dun Laoghaire, Ireland). PG4, standard cell culture medium and components were supplied by Sigma-Aldrich (Arklow, Ireland) and Bio-Sciences.

Animals and ethics statement. Pups from rats (Sprague Dawley) bred in an approved Bio-Resource Unit at Dublin City University were used. The experiments, maintenance and care of the rodents complied with the European Communities (Amendment of Cruelty to Animals Act 1876) Regulations 2002 and 2005. Experimental

procedures had been approved by the Research Ethics Committee of Dublin City University, and licenced by the Irish Health Products Regulatory Authority.

Constructs for recombinant BoNT/A variants. Experiments involving recombinant BoNTs had been approved by the Biosafety Committee of Dublin City University, and the Environmental Protection Agency of Ireland. To obtain $rA\Delta H_{CN}$, nucleotides encoding residues Ile_{874}-Q_{1091} were deleted with insertion of GGC GGT by inverted PCR, using a previously-reported pET29a-BoNT/A construct as template[19]. The resultant PCR products were self-ligated by T4 ligase and transformed into Top10 competent cells for screening of positive clones. In order to engineer rA-HA and $rA\Delta H_{CN}$-HA, a short nucleotide sequence encoding HA tag (YPYDVPDYA) was inserted before the thrombin recognition site located in the loop region of rA and $rA\Delta H_{CN}$. Constructs encoding BoNT/A with one or more mutated residues in the H_{CN} region were made by site-direct mutagenesis.

Production of recombinant toxins. After verifying all of the above constructs, plasmids were transformed into *E. coli* BL21.DE3 for expression, using an auto-induction medium[41]. Recombinant proteins were purified by IMAC on Talon resin. rA, $rA\Delta H_{CN}$ and their fusions with a HA tag were further purified by anion-exchange chromatography, following the protocol established for rA[19]. To activate the toxin, SC was incubated with thrombin (1 mg/1 unit of thrombin) at 22 °C for 1 h before adding phenylmethylsulfonyl fluoride to 1 mM concentration to stop the reaction. Protein concentration was quantified by Bradford reagent.

GST-SV2C-L4 pull down assay. GST-tagged $SV2C–L4_{(454–580)}$ protein (100 μg) was incubated with 50 μl of glutathione Sepharose (Fisher Scientific, Ballycoolin, Ireland) for 1 h at 4 °C. After washing with 1 ml of binding buffer[30,32], resin was incubated with different concentrations of rA, $rA\Delta H_{CN}$ or $rA(W_{985}L)$ DC in binding buffer. After washing 3 times with 1 ml of binding buffer, bound proteins were eluted by LDS sample buffer containing DTT with a final concentration of 50 mM. The reduced samples were analyzed by SDS-PAGE followed by Western blotting, using antibodies against LC/A or GST.

Measurements of protease activity, lethality and neuromuscular paralysis of the generated BoNTs. Proteolytic activities of rA, $rA\Delta H_{CN}$ and $rA(W_{985}L)$ were determined using a recombinant model substrate, green fluorescent protein (GFP)-SNAP25-C_{73}-His_6[27]. Briefly, the toxins were diluted to 50 nM in HBS-20 [20 mM HEPES, 100 mM NaCl, pH 7.4; 10 μg/ml bovine serum albumin (BSA); 5 mM DTT and 10 μM $ZnCl_2$]. This mixture was incubated at 37 °C for 30 min before a 2-fold serial dilution in HBS-20 and mixing with an equal volume of substrate (1 mg/ml). After further incubation for 30 min at 37 °C, reactions were stopped by adding ice-cold LDS sample buffer. Intact substrate and the larger BoNT-cleaved product were separated by SDS-PAGE (NuPAGE 12% precast Bis-Tris gel) and visualized by Coomassie staining.

The specific lethalities of rA and $rA\Delta H_{CN}$ were measured using a mouse lethality assay[28]. Briefly, this involved intraperitoneal injection into Tyler's Ordinary mice of several amounts of each toxin: 1–10 pg for rA, and 1–1000 ng for $rA\Delta H_{CN}$. The observed number of death within 5 days indicated the approximate lethalities; then, the assay was repeated by injecting 4 animals each with doses close to the expected LD_{50} (5–8 pg of rA, 100–500 ng of $rA\Delta H_{CN}$). The dose which killed half of each group was taken as a minimal LD_{50} value. Their relative abilities to induce neuromuscular paralysis were determined by the DAS values[29] recorded over time, following injection of the indicated amounts in 5 μl into the right gastrocnemius muscle of groups of 7 mice.

Primary culture of rat CGNs, TGNs and their treatment with BoNTs. Isolation and culture of CGNs and TGNs from 4–7 day old rats have been described previously[6,28]. Cultured neurons at 10–14 days *in vitro* (DIV) were incubated with various concentrations of each toxin in culture medium for 24 h before harvesting in LDS sample buffer. In one case, rat CGNs were incubated with BoNT/A or W985L mutant in low potassium (LK) buffer (mM: 20 HEPES, 120 NaCl, 5 KCl, 2 $MgCl_2$, 1.3 $CaCl_2$, and 5 glucose) for 8 min as described in ref. 16. After removing the unbound toxin by washes with DMEM, cells were further cultured in fresh medium for 5 h before harvesting in LDS sample buffer. Intact and BoNT-cleaved SNAP-25 were separated by SDS-PAGE (NuPAGE 12% precast Bis-Tris gel) and visualised by Western blotting, using an antibody recognizing both cleaved and intact forms. The proportion of intact SNAP-25 remaining was calculated relative to the total (cleaved plus remaining intact), using image J software analysis of digitised images.

Radio-iodination of BoNTs and their binding to CGNs. rA, $rA\Delta H_{CN}$ and $rA(W_{985}L)$ were iodinated using sodium ^{125}Iodine and a previously-described chloramine-T method with slight modification[33]. Briefly, each BoNT (40 μg in 40 μl) was added to 1 mCi (10 μl) of carrier free Na ^{125}I and derivatisation initiated by adding chloramine-T (5 μl of 2 mM to a final concentration of 0.22 mM). The reaction was quenched after 40 s by addition of an excess of L-tyrosine (25 μl of 1 mg/ml in 0.1 M sodium phosphate buffer pH 7.4 containing 150 mM NaCl). Free ^{125}I and tyrosine were separated from the ^{125}I-labelled toxin by gel filtration, using a PD-10 column equilibrated with the latter buffer. ^{125}I-toxins were stored at 4 °C in the presence of gelatin to a final concentration of 0.25% (w/v), following removal of aliquots to determine their specific radioactivities.

Cultured CGNs were suspended in PBS containing 1 mg/ml BSA. Aliquots (50–150 μg) were incubated with increasing concentrations of the ^{125}I-labelled toxin for 1 hour at 4 °C, or together with its unlabelled counterpart at ≥100-fold molar excess over the highest concentration of ^{125}I-toxin used. Binding was terminated by centrifugation (9,000× g for 2 min) and resuspension in ice-cold PBS, after which pellets were washed two further times as described prior to γ-counting.

Immuno-fluorescence staining. Rat TGNs grown on coverslips or μ -Slide 8-well Ibidi chambers (Ibidi GmbH, Martinsried, Germany) at 7 DIV were incubated with 100 nM rA, rA-HA or $rA\Delta H_{CN}$-HA for 24 h at 37 °C in culture medium. Cells were then washed three times with PBS before fixation with 3.7% paraformadehyde in

PBS for 30 minutes. The samples were then washed thrice with PBS, followed by permeabilisation for 5 minutes with 0.2% Triton X-100 in PBS before blocking with 1% BSA in PBS for 1 hour. A pair of primary antibodies [rabbit monoclonal anti-HA (1:1600) and mouse monoclonal anti-VAMP2 (1:1000)] were applied in the blocking solution for 1 hour at room temperature. Washed samples were incubated with fluorescent secondary antibodies (Alexa Fluor 488 goat anti-mouse IgG and Alexa Fluor 568 goat anti-rabbit IgG) for 1 hour. After five washes with PBS, the samples were then mounted with Vectashield (Vector Laboratories) and fluorescent images captured with an inverted Zeiss LSM 710 confocal microscope (Carl Zeiss Microimaging) using Zen2008 software (Universal Imaging, Göttingen).

Statistical analysis. Probability values were determined with the use of Student's unpaired two-tailed t-test or two-way ANOVA followed by Bonferroni post hoc test by GraphPad Prism software, as specified in figure legends. Values of $P < 0.05$ were considered significant.

References

1. Dolly, J. O., Wang, J., Zurawski, T. H. & Meng, J. Novel therapeutics based on recombinant botulinum neurotoxins to normalize the release of transmitters and pain mediators. *FEBS J* **278,** 4454–66 (2011).
2. Dorizas, A., Krueger, N. & Sadick, N. S. Aesthetic uses of the botulinum toxin. *Dermatol Clin* **32,** 23–36 (2014).
3. Hexsel, C., Hexsel, D., Porto, M. D., Schilling, J. & Siega, C. Botulinum toxin type A for aging face and aesthetic uses. *Dermatol Ther* **24,** 54–61 (2011).
4. Gady, J. & Ferneini, E. M. Botulinum toxin A and headache treatment. *Conn Med* **77,** 165–6 (2013).
5. Welch, M. J., Purkiss, J. R. & Foster, K. A. Sensitivity of embryonic rat dorsal root ganglia neurons to Clostridium botulinum neurotoxins. *Toxicon* **38,** 245–58 (2000).
6. Meng, J., Wang, J., Lawrence, G. & Dolly, J. O. Synaptobrevin I mediates exocytosis of CGRP from sensory neurons and inhibition by botulinum toxins reflects their anti-nociceptive potential. *J Cell Sci* **120,** 2864–74 (2007).
7. Durham, P. L., Cady, R. & Cady, R. Regulation of calcitonin gene-related peptide secretion from trigeminal nerve cells by botulinum toxin type A: implications for migraine therapy. *Headache* **44,** 35–42, discussion 42-3 (2004).
8. Meng, J., Wang, J., Steinhoff, M. & Dolly, J. O. TNFalpha induces co-trafficking of TRPV1/TRPA1 in VAMP1-containing vesicles to the plasmalemma via Munc18-1/syntaxin1/SNAP-25 mediated fusion. *Sci Rep* **6,** 21226, 1–15 (2016).
9. Lacy, D. B., Tepp, W., Cohen, A. C., DasGupta, B. R. & Stevens, R. C. Crystal structure of botulinum neurotoxin type A and implications for toxicity. *Nat Struct Biol* **5,** 898–902 (1998).
10. Kumaran, D. *et al.* Domain organization in Clostridium botulinum neurotoxin type E is unique: its implication in faster translocation. *J Mol Biol* **386,** 233–45 (2009).
11. Swaminathan, S. & Eswaramoorthy, S. Structural analysis of the catalytic and binding sites of Clostridium botulinum neurotoxin B. *Nat Struct Biol* **7,** 693–9 (2000).
12. Dolly, J. O., Black, J., Williams, R. S. & Melling, J. Acceptors for botulinum neurotoxin reside on motor nerve terminals and mediate its internalization. *Nature* **307,** 457–60 (1984).
13. Jin, R., Rummel, A., Binz, T. & Brunger, A. T. Botulinum neurotoxin B recognizes its protein receptor with high affinity and specificity. *Nature* **444,** 1092–5 (2006).
14. Chai, Q. *et al.* Structural basis of cell surface receptor recognition by botulinum neurotoxin B. *Nature* **444,** 1096–100 (2006).
15. Black, J. D. & Dolly, J. O. Interaction of 125I-labeled botulinum neurotoxins with nerve terminals. I. Ultrastructural autoradiographic localization and quantitation of distinct membrane acceptors for types A and B on motor nerves. *J Cell Biol* **103,** 521–34 (1986).
16. Meng, J., Wang, J., Lawrence, G. W. & Dolly, J. O. Molecular components required for resting and stimulated endocytosis of botulinum neurotoxins by glutamatergic and peptidergic neurons. *FASEB J* **27,** 3167–80 (2013).
17. Montal, M. Botulinum neurotoxin: a marvel of protein design. *Annu Rev Biochem* **79,** 591–617 (2010).
18. Pirazzini, M. *et al.* Thioredoxin and its reductase are present on synaptic vesicles, and their inhibition prevents the paralysis induced by botulinum neurotoxins. *Cell Rep* **8,** 1870–8 (2014).
19. Wang, J. *et al.* A dileucine in the protease of botulinum toxin A underlies its long-lived neuroparalysis: transfer of longevity to a novel potential therapeutic. *J Biol Chem* **286,** 6375–85 (2011).
20. Jacky, B. P. *et al.* Identification of fibroblast growth factor receptor 3 (FGFR3) as a protein receptor for botulinum neurotoxin serotype A (BoNT/A). *PLoS Pathog* **9,** e1003369 (2013).
21. Sun, S. *et al.* Receptor binding enables botulinum neurotoxin B to sense low pH for translocation channel assembly. *Cell Host Microbe* **10,** 237–47 (2011).
22. Benoit, R. M. *et al.* Structural basis for recognition of synaptic vesicle protein 2C by botulinum neurotoxin A. *Nature* **505,** 108–11 (2014).
23. Yao, G. *et al.* N-linked glycosylation of SV2 is required for binding and uptake of botulinum neurotoxin A. *Nat Struct Mol Biol* (2016).
24. Lacy, D. B. & Stevens, R. C. Sequence homology and structural analysis of the clostridial neurotoxins. *J Mol Biol* **291,** 1091–104 (1999).
25. Muraro, L., Tosatto, S., Motterlini, L., Rossetto, O. & Montecucco, C. The N-terminal half of the receptor domain of botulinum neurotoxin A binds to microdomains of the plasma membrane. *Biochem Biophys Res Commun* **380,** 76–80 (2009).
26. Zhang, Y. *et al.* Structural insights into the functional role of the Hcn sub-domain of the receptor-binding domain of the botulinum neurotoxin mosaic serotype C/D. *Biochimie* **95,** 1379–85 (2013).
27. Fernandez-Salas, E. *et al.* Plasma membrane localization signals in the light chain of botulinum neurotoxin. *Proc Natl Acad Sci USA* **101,** 3208–13 (2004).
28. Wang, J. *et al.* Novel chimeras of botulinum neurotoxins A and E unveil contributions from the binding, translocation, and protease domains to their functional characteristics. *J Biol Chem* **283,** 16993–7002 (2008).
29. Aoki, K. R. A comparison of the safety margins of botulinum neurotoxin serotypes A, B, and F in mice. *Toxicon* **39,** 1815–20 (2001).
30. Dong, M. *et al.* SV2 is the protein receptor for botulinum neurotoxin A. *Science* **312,** 592–6 (2006).
31. Dong, M. *et al.* Glycosylated SV2A and SV2B mediate the entry of botulinum neurotoxin E into neurons. *Mol Biol Cell* **19,** 5226–37 (2008).
32. Meng, J. *et al.* Activation of TRPV1 mediates calcitonin gene-related peptide release, which excites trigeminal sensory neurons and is attenuated by a retargeted botulinum toxin with anti-nociceptive potential. *J Neurosci* **29,** 4981–92 (2009).
33. Williams, R. S., Tse, C. K., Dolly, J. O., Hambleton, P. & Melling, J. Radioiodination of botulinum neurotoxin type A with retention of biological activity and its binding to brain synaptosomes. *Eur J Biochem* **131,** 437–45 (1983).
34. Chaddock, J. A. *et al.* A conjugate composed of nerve growth factor coupled to a non-toxic derivative of Clostridium botulinum neurotoxin type A can inhibit neurotransmitter release *in vitro*. *Growth Factors* **18,** 147–55 (2000).
35. Duggan, M. J. *et al.* Inhibition of release of neurotransmitters from rat dorsal root ganglia by a novel conjugate of a Clostridium botulinum toxin A endopeptidase fragment and Erythrina cristagalli lectin. *J Biol Chem* **277,** 34846–52 (2002).

36. Arsenault, J. *et al.* Stapling of the botulinum type A protease to growth factors and neuropeptides allows selective targeting of neuroendocrine cells. *J Neurochem* **126,** 223–33 (2013).
37. Masuyer, G., Chaddock, J. A., Foster, K. A. & Acharya, K. R. Engineered botulinum neurotoxins as new therapeutics. *Annu Rev Pharmacol Toxicol* **54,** 27–51 (2014).
38. Somm, E. *et al.* A botulinum toxin-derived targeted secretion inhibitor downregulates the GH/IGF1 axis. *J Clin Invest* **122,** 3295–306 (2012).
39. Dressler, D. Clinical features of antibody-induced complete secondary failure of botulinum toxin therapy. *Eur Neurol* **48,** 26–9 (2002).
40. Lange, O. *et al.* Neutralizing antibodies and secondary therapy failure after treatment with botulinum toxin type A: much ado about nothing? *Clin Neuropharmacol* **32,** 213–8 (2009).
41. Studier, F. W. Protein production by auto-induction in high density shaking cultures. *Protein Expr Purif* **41,** 207–34 (2005).

Acknowledgements

The authors thank Drs. M. Brin, A. Brideau-Andersen and B. Jacky for their general comments on this manuscript, and Allergan Inc for part funding. This research is supported by a PI grant (09/IN.1/B2634 to JOD) and a Career Development Award (13/CDA/2093 to JW) from Science Foundation Ireland.

Author Contributions

J.W. and J.M. devised the study; J.W., J.M., M.N. and M.T. performed the experiments; J.W., J.M., and J.O.D. interpreted the results; J.W., J.M. and M.N. prepared the figures; J.W., J.M. and M.N. drafted the manuscript; J.W., J.M. and J.O.D. revised the paper.

Additional Information

Supplementary information accompanies this paper at http://www.nature.com/srep

Competing Interests: The authors declare that this research was supported in part by Allergan Inc. The funder had no role in study design, data collection and analysis or preparation of the manuscript.

How to cite this article: Wang, J. *et al.* Neuronal entry and high neurotoxicity of botulinum neurotoxin A require its N-terminal binding sub-domain. *Sci. Rep.* **7**, 44474; doi: 10.1038/srep44474 (2017).

Publisher's note: Springer Nature remains neutral with regard to jurisdictional claims in published maps and institutional affiliations.